

# COMPARISON OF MODEL PREDICTIVE CURRENT CONTROLLERS FOR GRID-TIED INVERTERS

Jordan Pauleski Zucuni, Humberto Pinheiro, Fernanda de Moraes Carnielutti, Paulo Jefferson Dias de Oliveira Evald  
Federal University of Santa Maria  
Santa Maria, Rio Grande do Sul

Power Electronics and Control Research Group - GEPOC

Email: jzucuni@gmail.com, humberto.ctlab.ufsm.br@gmail.com, fernanda.carnielutti@gmail.com, paulo.evald@gmail.com

**Abstract**—This paper compares two model predictive current control techniques for grid-tied inverters. The first one uses a single switching vector in a sampling period which results in a variable switching frequency, while the second technique operates with constant switching frequency. Both techniques have been implemented in a DSP + FPGA setup. The results demonstrated that both techniques have very fast transient response. Although the later demands a higher computational effort, it also improves significantly the harmonic spectrum since it concentrates the PWM harmonics around the sampling frequency. It has been found that during the transitions between two sectors of space vector diagram there are disturbances on the current which are relevant when operating with small output filters. Experimental results using Hardware In The Loop are presented to demonstrate the performance of the considered model predictive current controllers.

**Keywords** – Grid-tied PWM Inverters, Model Predictive Current Control, Space Vector Modulation

## I. INTRODUCTION

Model Predictive Control (MPC) has been a topic of research for more than three decades [1] and has received a lot of attention in power electronics [2]–[6]. It basically consists of using explicitly the mathematical model of the system to predict future values of variables in order to evaluate a cost function that express the desired behavior of the system over a defined horizon of time, usually denoted in terms of time samplings. The control action is then selected as being the input that minimizes that cost function [7].

The cost function can have as many terms as desired, involving the objectives of the control designer such as reference tracking and capacitor voltage balancing [8] or any other optimization feature required as number of switch transitions. It is important to note that the cost function is solved in a open loop basis. However it is recalculated at each sampling instant, updating the predictions with the new state of the system. This process is called receding horizon principle. Eventually, depending on the considered horizon, a sequence of inputs are generated. In this case, only the first element is applied to the system.

MPC can be classified according to the type of optimization problem [7], being divided into two generic groups: Continuous Control Set MPC (CCS-MPC) and Finite Control Set MPC (FCS-MPC). In the former, a continuous signal is computed and then applied to a subsequent modulator stage which can be any conventional one [7]. The later take into account the discrete nature of the converter, making a finite control set search of the solution through the selection of the switching vector that returns the lowest cost function.

FCS-MPC still according to [7] can be subdivided into two groups: Optimal Switching Vector MPC (OSV-MPC) and Optimal Switching Sequence MPC (OSS-MPC). The difference between them is the number of vectors that are applied in one sampling time  $T_s$ . OSV-MPC refers to the application of only one vector in one  $T_s$ , while OSS-MPC employs a sequence of vectors which resembles a conventional modulator.

The concept of OSV-MPC is cleared explained in [3], which demonstrates the application of MPC in power electronics. In this paper, the finite control set of inputs is composed of all possible converter switching vectors. From this set, only one vector is selected in order to minimize a given cost function. This turns out to be a very intuitive and a simple way to control the output currents of a 2-level 3-phase inverter. However only one vector is applied in a sampling period  $T_s$ . Besides, the same vector can be selected continuously for more than one sampling period. As a consequence, it can result in a low and variable switching frequency.

In order to overcome this drawback, [9] presented an OSS-MPC technique called Modulated Model Predictive Control ( $M^2PC$ ), which reorganizes the FCS-MPC method into a Space Vector Modulation (SVM) structure. Basically, the vectors are arranged in sectors, just as in SVM, but the costs are assigned to the sectors. Thus it is not the vector by itself that is selected as in OSV-MPC case, but the sector that returns the lowest cost. The manner in which the vectors are distributed during a sampling period  $T_s$  can be any one. In this way, fixed switching frequency can be achieved while keeping the advantages of FCS-MPC such as intuitive formulation, ability to easily develop multiobjective solutions and inclusion of

nonlinearities in a straight manner [9].

A well-known disadvantage of FCS-MPC is the computational burden for its implementation [7]. It was just with the development of more powerful processors that the implementation of FCS-MPC strategies in power electronics became feasible. However, the computational effort is still significant for the implementation of FCS-MPC strategies even with the nowadays hardware, specially if the method shows some complexity [10]. As a consequence, it turns out that the computational effort is a key factor when considering a FCS-MPC strategy.

Therefore, an evaluation concerning the benefits of M<sup>2</sup>PC against OSV-MPC considering mainly the computational burden and the harmonic content of the output current is valuable for practical reasons. In order to quantify the performance of MPC algorithms, this paper presents a comparison between the OSV-MPC technique presented in [3] and the OSS-MPC presented in [9] for a 2-level 3-phase inverter.

## II. DESCRIPTION OF THE INVERTER

In this section, the well-known 2-level 3-phase grid-tied inverter is described, Figure 1. This is the topology used for the implementation of the two techniques described in this work. The reason of this choice is based on the simplicity of the inverter and due to the fact of being a popular and widely used topology in many distributed generation applications.

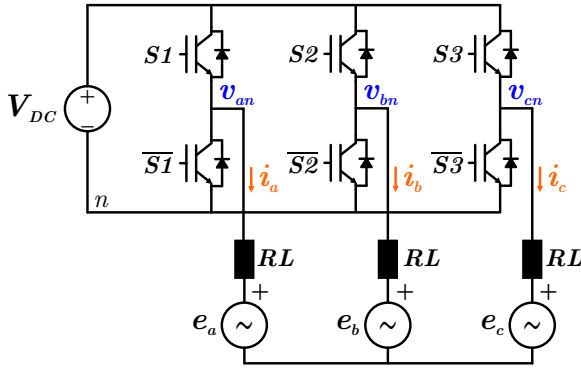


Figure 1. 2-level 3-phase grid-tied inverter

Each leg contains two complementary switches with the corresponding output phase voltage (with respect to the point  $n$ ) being 0 V or  $V_{DC}$ . In Table I, all possible switching states with the corresponding output phase voltages in alpha-beta frame are presented.

Figure 2 shows the Space Vector (SV) diagram for the 2-level 3-phase inverter. It is important to note that in this case there is a redundancy for the null vector, i.e., two different switching vectors generates the same  $\alpha\beta$  phase voltage. It can be observed from Table I looking at the first and the last row. Each triangle in Figure 2 is called a sector and is denominated by the number inside it.

Table I  
SWITCHING STATES FOR A 2-LEVEL 3-PHASE INVERTER

Index	$S_1$	$S_2$	$S_3$	$V_\alpha$	$V_\beta$
0	0	0	0	0	0
1	0	0	1	$-1/3$	$-\sqrt{3}/2$
2	0	1	0	$-1/3$	$\sqrt{3}/2$
3	0	1	1	$-2/3$	0
4	1	0	0	$2/3$	0
5	1	0	1	$1/3$	$-\sqrt{3}/2$
6	1	1	0	$1/3$	$\sqrt{3}/2$
7	1	1	1	0	0

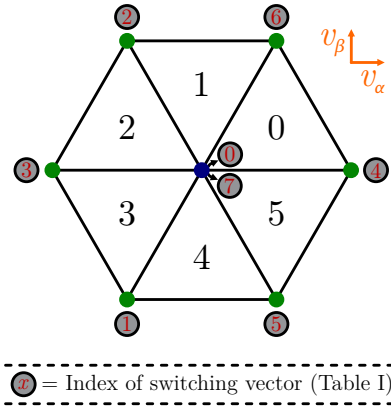


Figure 2. Space vector diagram for a 2-level 3-phase inverter

Considering alpha-beta reference frame, the output currents can be modeled by:

$$\frac{di_{\alpha,\beta}}{dt} = \frac{1}{L} (-Ri_{\alpha,\beta} + v_{\alpha,\beta} - e_{\alpha,\beta}) \quad (1)$$

Equation 1 can be discretized, considering a sampling time  $T_s$ , by Euler approximation, resulting:

$$i_{\alpha,\beta}[k+1] = i_{\alpha,\beta}[k] + \frac{T_s}{L} (-Ri_{\alpha,\beta}[k] + v_{\alpha,\beta}[k] - e_{\alpha,\beta}[k]) \quad (2)$$

or in a compact form:

$$x[k+1] = ax[k] + b(v[k] - e[k]) \quad (3)$$

where  $a = 1 - \frac{RT_s}{L}$  and  $b = \frac{T_s}{L}$ .

The two MPC strategies can be implemented by the use of equation 2. For each of the 8 switching vectors, a cost function that involves the current tracking is evaluated (see equation 4). These strategies are described in the following sections.

## III. STRATEGY 1: FCS-OSV MPC

In this strategy, which the principle is presented in [3], at each sampling period, the following cost function for the  $i^{th}$  vector is evaluated, just like found in [9]:

$$g_i = \|i^* - x_i^p\|^2, \quad i \in \{0...7\} \quad (4)$$

where  $i^*$  and  $x_i^p$  represents the current reference and the predicted current at the  $k+1$  sampling period, respectively. Once all of the 8 costs are evaluated, a routine selects the vector that results in the lowest cost, applying it to the converter for the entire sampling period  $T_s$ .

In the next sampling time, the same procedure is repeated with the updated values of state variables. The criterion for the vector selection is based only on the  $g_i, i \in \{0...7\}$  value. As a consequence, the vectors are selected erratically over a window of sampling periods. For instance, the same vector can be applied in more than one period. It implies in a non-fixed switching frequency and in a spread output harmonic content which will be demonstrated in section V.

This is a very simple and intuitive approach that can include multiobjective solutions resembling an optimization problem through the use of a cost function, which can include more terms and constraints with the objective of, for example, avoiding the use of the same vector consecutively or making a balance of the number of commutations among power switches.

#### IV. STRATEGY 2: FCS M<sup>2</sup>PC

In this strategy, which the principle is presented in [9], the same cost function presented in equation 4 is also evaluated for each of the 8 vectors. However, instead of directly select the vector that minimizes the cost function to be applied to the converter, a cost is associated with each sector of the Space Vector (SV) diagram. The sector with the lowest cost is selected to be applied to the inverter and the vector sequence can be any one as long as each one of the three vectors of the selected sector appears at least once within the sampling period  $T_s$ . In this work, the following sequence has been adopted:

$$S = \{S_0, S_1, S_2, S_1, S_0\} \quad (5)$$

where  $S_0$  has been selected as  $[0 \ 0 \ 0]^T$ ,  $S_1$  is the first active vector found when traversing the SV diagram on the counterclockwise direction, and  $S_2$  is the other active vector of the sector under consideration.

To calculate the mentioned cost for the  $j^{th}$  sector, [9] derive equations based on the minimization of the root-mean-square (RMS) value of the costs weighted by the corresponding duty cycles, finding the solution through Karush–Kuhn–Tucker conditions. The following equations were utilized in the order that is presented (for more details see [9]).

$$Q_j = \frac{1}{\sum g_{ji}^{-1}} \quad (6)$$

$$d_{ji} = \frac{Q_j}{g_{ji}} \quad (7)$$

$$G_j = \sum g_{ji} d_{ji}^2 \quad (8)$$

For the above equations, the generic variable  $x_{ji}$  means the  $i^{th}$  vector of the  $j^{th}$  sector. The term  $Q_j$  is introduced in the mathematical solution, the cost  $g_{ji}$  is the same of equation 4, the variable  $d_{ji}$  refers to the duty cycle of the corresponding vector and  $G_j$  is the cost of the sector.

As the three switching vectors of a sector are always applied in one  $T_s$ , this strategy provides fixed switching frequency while keeps the MPC logic approach.

#### V. DELAY COMPENSATION

In practical implementations, it is impossible, right at the sampling instant  $k$ , acquire the measured variables, run the control routine and apply the output to the inverter, as long as each of this processes takes a share of time. Thus the output calculated at sampling instant  $k$  will be effectively applied in  $k+1$ . As a consequence, the predictive control is calculated from  $k+1$  to  $k+2$  sampling period.

It turns out that the necessary values of the variables at  $k+1$  to the prediction must be estimated, as well as the reference value at  $k+2$ . In order to that, the estimation in  $k+1$  is made using the same equation 2, but considering the vectors applied in the corresponding previous sampling period. As long as  $T_s$  is sufficiently small, both the future reference as the grid voltage values can be considered to be known.

#### VI. EXPERIMENTAL RESULTS

In this section, the experimental results will be presented showing the waveforms of the output currents, the spectrum content and the necessary time to run the control routine. The practical setup has a Typhoon HIL402, a TEXAS TMS320F28335 DSP and a Xilinx<sup>®</sup> Spartan<sup>®</sup> 3E-500 FPGA. While the Typhoon HIL emulated the 2-level 3-phase inverter, the DSP executed the control routine and the FPGA worked as a space vector modulator to apply the switching sequences with the corresponding duty cycles. The parameters used for the inverter is presented in Table II.

Table II  
PARAMETERS FOR PRACTICAL IMPLEMENTATION

Parameter	Description	Value
$P$	Nominal Power	50 kW
$V_{DC}$	DC Bus Voltage	800 V
$e_a, e_b, e_c$	Grid Phase Voltages	220 V (RMS Value)
$R$	Output Filter Resistance	0.5 $\Omega$
$L$	Output Filter Inductance	5 mH
$T_s$	Sampling Period	100 $\mu s$ ; 30 $\mu s$
$i_g^*$	Grid Current Reference	100 A (peak current)

In the following, the output currents waveforms are shown. The duration for the algorithm execution for each strategy is presented in Table III.

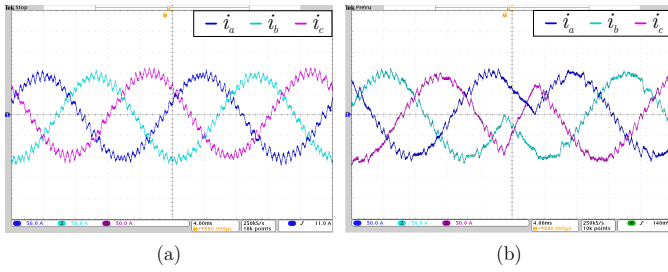


Figure 3. Strategy 1,  $T_s = 100 \mu s$ : (a) Output currents. (b) Transient response for a  $180^\circ$  phase shift on the reference.

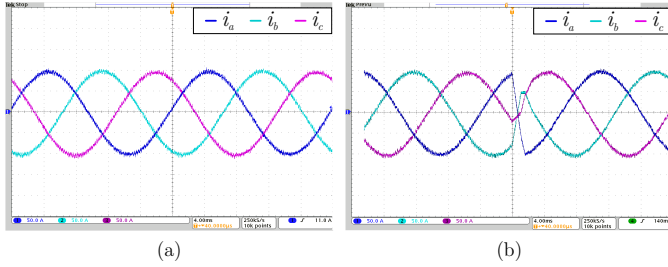


Figure 4. Strategy 1,  $T_s = 30 \mu s$ : (a) Output currents. (b) Transient response for a  $180^\circ$  phase shift on the reference.

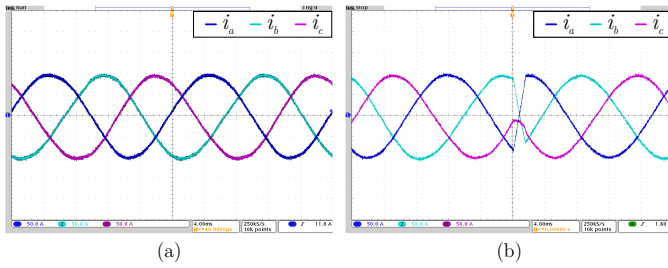


Figure 5. Strategy 2,  $T_s = 100 \mu s$ : (a) Output currents. (b) Transient response for a  $180^\circ$  phase shift on the reference.

Table III  
COMPUTATIONAL TIME

Strategy 1: FCS-OSV MPC	22 $\mu s$
Strategy 2: FCS M <sup>2</sup> PC	62 $\mu s$

As can be seen from Figure 3 to 5, both MPC techniques tracks satisfactory the current reference and show very good transient responses. It can be observed that due to the fact that strategy 1 applies only one vector per sampling period, the current ripple is very pronounced when using relatively low  $T_s$  values even with a large filter inductor. However, as the computational effort is lower,  $T_s$  can be reduced, as long as it does not compromise the switching losses.

The strategy 2: FCS M<sup>2</sup>PC, on the other hand, presents much higher computational effort but as five vectors are applied (see eq. 5) the resulting current has smaller current ripple. In figure 6, a comparison regarding harmonic content for the three cases are presented.

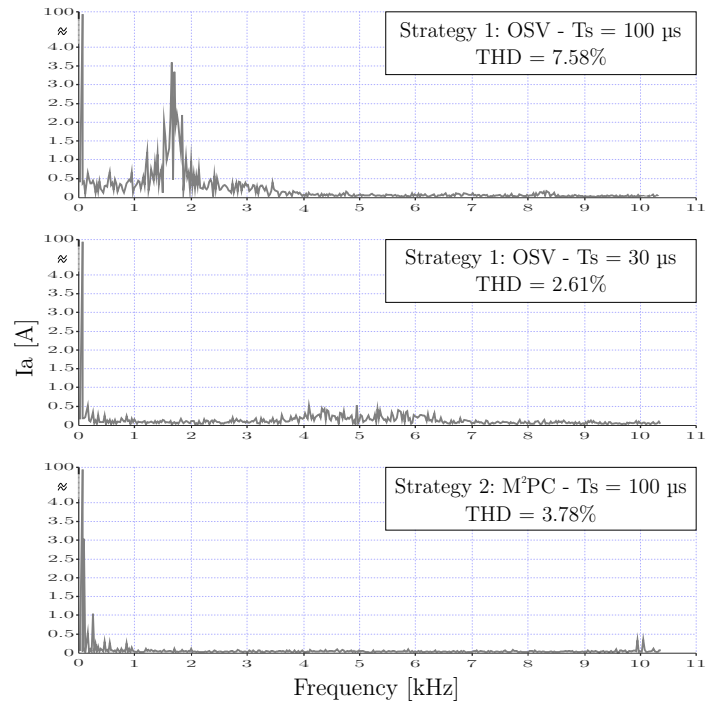


Figure 6. Spectrum for the three cases considered

From figure 6, it can be seen that the OSV technique shows a widespread spectrum, while the M<sup>2</sup>PC technique shows harmonics concentrated around the sampling frequency. However, it also has low order harmonics. This is observed in the waveform specially when the inductor filter is reduced, for example, in Figure 7,  $L = 500 \mu H$ .

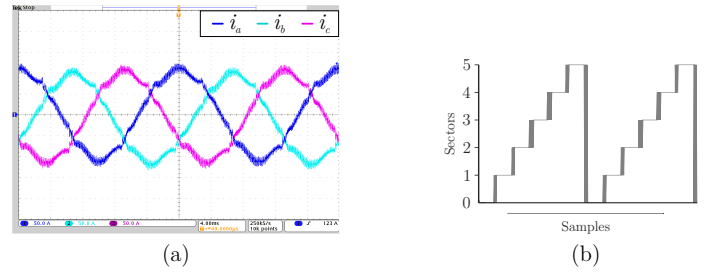


Figure 7. (a) Output current when  $L = 500 \mu H$ ,  $T_s = 100 \mu s$ . (b) The way in which the algorithm selects the sectors.

Analyzing Figure 7, it can be seen that close to the boundaries between sectors there is a chattering. As a result, it is possible to see a distortion on the current. So, further research is needed to clarify and overcome this limitation.

## VII. CONCLUSIONS

This article compares two strategies of finite control set model predictive current control for a 2-level 3-phase inverter. The first one is the OSV technique and the second one is the M<sup>2</sup>PC technique. The main difference between the two is the number of vectors applied in a sample period.

It can be concluded that the OSV-MPC takes a significantly lower computational effort which allows the sampling period  $T_s$  to be reduced as long as it does not compromise switching losses. On the other hand, this technique shows a widespread spectrum while M<sup>2</sup>PC resembles a conventional modulator with concentration of the harmonics around the sampling frequency, showing lower current ripple for the same sampling period  $T_s$ . However, there is a chattering close to the boundaries of sectors. At this point, further research are needed to address this issue.

#### REFERENCES

- [1] J. H. Lee, "Model predictive control: Review of the three decades of development," *International Journal of Control, Automation and Systems*, vol. 9, no. 3, p. 415, Jun 2011. [Online]. Available: <https://doi.org/10.1007/s12555-011-0300-6>
- [2] S. A. Larrinaga, M. A. R. Vidal, E. Oyarbide, and J. R. T. Apraiz, "Predictive control strategy for dc/ac converters based on direct power control," *IEEE Transactions on Industrial Electronics*, vol. 54, no. 3, pp. 1261–1271, June 2007.
- [3] J. Rodriguez, J. Pontt, C. A. Silva, P. Correa, P. Lezana, P. Cortes, and U. Ammann, "Predictive current control of a voltage source inverter," *IEEE Transactions on Industrial Electronics*, vol. 54, no. 1, pp. 495–503, Feb 2007.
- [4] X. Cai, Z. Zhang, J. Wang, and R. Kennel, "Optimal control solutions for pmsm drives: A comparison study with experimental assessments," *IEEE Journal of Emerging and Selected Topics in Power Electronics*, vol. 6, no. 1, pp. 352–362, March 2018.
- [5] J. Rodriguez, M. P. Kazmierkowski, J. R. Espinoza, P. Zanchetta, H. Abu-Rub, H. A. Young, and C. A. Rojas, "State of the art of finite control set model predictive control in power electronics," *IEEE Transactions on Industrial Informatics*, vol. 9, no. 2, pp. 1003–1016, May 2013.
- [6] Y. Zhang and Y. Peng, "Performance evaluation of direct power control and model predictive control for three-level ac/dc converters," in *2015 IEEE Energy Conversion Congress and Exposition (ECCE)*, Sept 2015, pp. 217–224.
- [7] S. Vazquez, J. Rodriguez, M. Rivera, L. G. Franquelo, and M. Norambuena, "Model predictive control for power converters and drives: Advances and trends," *IEEE Transactions on Industrial Electronics*, vol. 64, no. 2, pp. 935–947, Feb 2017.
- [8] T. Geyer, R. P. Aguilera, and D. E. Quevedo, "On the stability and robustness of model predictive direct current control," in *2013 IEEE International Conference on Industrial Technology (ICIT)*, Feb 2013, pp. 374–379.
- [9] F. Donoso, A. Mora, R. Cárdenas, A. Angulo, D. Sáez, and M. Rivera, "Finite-set model-predictive control strategies for a 3l-npc inverter operating with fixed switching frequency," *IEEE Transactions on Industrial Electronics*, vol. 65, no. 5, pp. 3954–3965, May 2018.
- [10] S. Kouro, M. Perez, J. Rodriguez, A. Llor, and H. Young, "Model predictive control: Mpc's role in the evolution of power electronics," vol. 9, pp. 8–21, 12 2015.